The Journal of Experimental Biology 204, 1687–1696 (2001)
Printed in Great Britain © The Company of Biologists Limited 2001
JEB 3087

LIFT-BASED PADDLING IN DIVING GREBE

L. CHRISTOFFER JOHANSSON* AND ULLA M. LINDHE NORBERG
Department of Zoology, Göteborg University, Box 463, SE-405 30 Göteborg, Sweden
*e-mail: christoffer.johansson@zool.gu.se

Accepted 26 February; published on WWW 23 April 2001

Summary

To examine the hydrodynamic propulsion mechanism of a diving great crested grebe (*Podiceps cristatus*), the three-dimensional kinematics was determined by digital analysis of sequential video images of dorsal and lateral views. During the acceleration phase of this foot-propelled bird, the feet move through an arc in a plane nearly normal to the bird's line of motion through the water, i.e. the toes move dorsally and medially but not caudally relative to the water. The kinematics of the grebe's lobed feet is different from that in anseriforms, whose feet move in a plane mostly parallel to the bird's line of progress through the water. Our results suggest that the foot-propelled locomotor mechanism of grebes is based primarily on a lift-producing leg and foot stroke, in contrast to the drag-based locomotion assumed previously. We suggest that the lift-based paddling of grebes considerably increases both maximum swimming speed and energetic efficiency over drag-based propulsion. Furthermore, the results implicate a new interpretation of the functional morphology of these birds, with the toes serving as a self-stabilizing multi-slotted hydrofoil during the power phase.

Key words: great crested grebe, *Podiceps cristatus*, paddling, lift production, kinematics, hydrofoil, multislots, diving, swimming, hydrodynamics.

Introduction

Diving birds, in particular foot-propelled ones, can be separated into different groups on the basis of their underwater foraging behaviour (Cramp and Simmons, 1983; Harper et al., 1985). Birds that feed on benthic organisms (plants, mussels, etc.) merely swim under water to a fixed foraging patch, whereas piscivores actively pursue their swimming prey (fish). An interesting question is whether there are unique features of the locomotor mechanism of foot-propelled divers that vigorously chase their prey compared with those that graze on immobile food. Another question is what selection pressures may have acted on fish-eating birds that distinguish them from benthivores. One obvious factor is the need for speed, since chasing fish requires high velocity. Another probable factor is the need for an energy-efficient propulsion mechanism, since pursuing fish probably requires a higher swimming speed, and thus more energy, than does diving to graze. Both increased speed and increased efficiency at high speed favour a lift-based propulsion mechanism (Fish, 1996).

Most previous studies have focused on underwater locomotor mechanisms and behaviour in grazing anseriforms (Lovvorn et al., 1991; Lovvorn, 1994; Stephenson, 1994; Carbone et al., 1996), but little is known about the functional morphology and kinematics of underwater locomotion in foot-propelled diving birds (Townsend, 1909; Dabelow, 1925; Brooks, 1945; Tome and Wrubleski, 1988). Even within anseriforms, previous investigations have focused not on the kinematics of the birds' propulsors but rather on the energetics of swimming and on the changes in buoyancy with changes in diving depth (Stephenson et al., 1989; Lovvorn and Jones, 1991; Stephenson, 1994; Carbone et al., 1996). Few groups other than anseriforms have been studied (Frank and Nue, 1929; Nue, 1931) and, to our knowledge, the kinematics of a diving grebe (Podicipediformes) has been studied only by Frank and Nue (Frank and Nue, 1929). Their kinematic description is insufficient to draw any conclusions about the hydrodynamic mechanisms of propulsion.

There is large variation in the foot and leg morphology of diving birds using foot propulsion (Högman, 1873; Wilcox, 1952; Owre, 1967; Raikow, 1970; Rosser et al., 1982). Some of the most specialized foot-propelled birds are the Podicipediformes, Gaviiformes and the extinct Hesperornithiformes, which morphologically form a rather homogeneous group (Högman, 1873; Dabelow, 1925; Cracraft, 1982) that have a short femur and a long tibiotarsus and tarsometatarsus compared with other diving birds (L. C. Johansson, personal observation). Furthermore, the toe morphology of grebes is unique among extant birds. Each toe has separate and rather stiff skin lobes enlarging the toe surface, and only the inner parts of the toes are fused by webbing. The lobing is asymmetrical, with the lateral lobe on each toe being smaller than the medial one (Stolpe, 1935). Stolpe suggested that this asymmetrical lobing is an adaptation for increasing drag during the power stroke and reducing drag during the recovery stroke. However, we have shown that a

more sophisticated function is possible (Johansson and Lindhe Norberg, 2000). The toes might function as multiple slots during swimming, which would increase the efficiency of the power stroke. A condition for this is that the propulsion mechanism is lift-based.

We studied the kinematics of a diving piscivorous bird, the great crested grebe (*Podiceps cristatus*), to investigate the hydrodynamics of its propulsive mechanism and to determine whether the propulsion is lift-based. We also studied the morphology of the legs and feet of the grebe as a basis for functional interpretations.

Materials and methods

Animals

The experiment was conducted using a 1-year-old great crested grebe (*Podiceps cristatus* L.) raised from an egg in captivity and fed on live and frozen fish. From early on, the bird had the opportunity to swim daily, and during the 8 months before the study it spent at least 8 h a day in water and was allowed to exit and enter the water at will.

Morphometrics

The following measurements were made: the length of the tarsometatarsus (the distance between the condyle of the third toe and the hypotarsus), the width/depth ratio at the middle of the tarsometatarsus, foot area (the areas of toes II, III and IV) and toe length (the distance from the condyle on the tarsometatarsus to the tip of the toe). A vernier caliper was used for the leg variables, whereas foot area and toe lengths were measured from photographs using Scion Image. Toe asymmetry was measured at 75 % of the toe length and was taken as the distance from the leading edge to the centre of the bone element of the toe divided by the chord of the toe (the distance from the leading edge of the toe to the trailing edge of the lobe).

Experimental arrangement

The bird was filmed in a swimming pool with a diameter of 4.6 m and a depth of 1.3 m. The filming was conducted using two Hi-8 video cameras, one submerged in an underwater house (lateral view) and one above the water surface (dorsal view). The bird was trained to dive through a mesh tunnel 2 m long, 0.40 m high and 0.60 m wide. The tunnel had a 1 m long measuring section in the middle consisting of a grid of 0.05 m×0.05 m and with its bottom surface 0.40 m above the bottom of the pool. The distance from the middle of the tunnel to any solid wall was at least 0.55–0.60 m. The dorsal view was filmed *via* a mirror, placed at 45 ° to the surface; we eliminated the refraction effect of waves by placing a box with a glass bottom above the tunnel submerged to approximately 0.02 m.

Image analysis

The video sequences were captured using a FAST Moviemachine II framegrabber. Of 172 captured sequences (sets of both dorsal and lateral views), 32 sequences (sets of both dorsal and lateral views) were considered useful, i.e. the bird was swimming straight and at a fairly constant speed (no apparent acceleration or deceleration). Of these 32 sequences, 13 of the best (with symmetrical strokes and a straight swimming path seen from both the dorsal and lateral view) were chosen for the analysis. The pictures were separated into frames (resulting in a speed of 50 frames s^{-1}) and contrast-enhanced with the use of Adobe Photoshop 4.0. The resulting stacks of frames were then analysed using Scion Image.

In addition to a point of reference on the tunnel wall, six marks were digitized on each frame for both the dorsal and lateral views, one on the tip of the tail (Tail) and five on the leg closest to the lateral camera: the joint between the tibiotarsus and tarsometatarsus (Tbt-Tmt), the joint between the tarsometatarsus and the foot (Tmt-Foot) and the tip of each of the three largest toes (toes II, III and IV) (Fig. 1). The tail-tip (Tail) was taken as a fixed body point because it was easily distinguishable in both the dorsal and lateral views.

Filming from the dorsal and lateral views allowed elimination of parallax, which was performed after adjusting for any tilt of the camera.

Data analysis

The mean swimming speed of the bird was calculated as the mean distance travelled during an entire paddling cycle divided by the period of the stroke. This speed was used to calculate the Reynolds number (*Re*; $Re=lV/\nu$, where l is length, V is

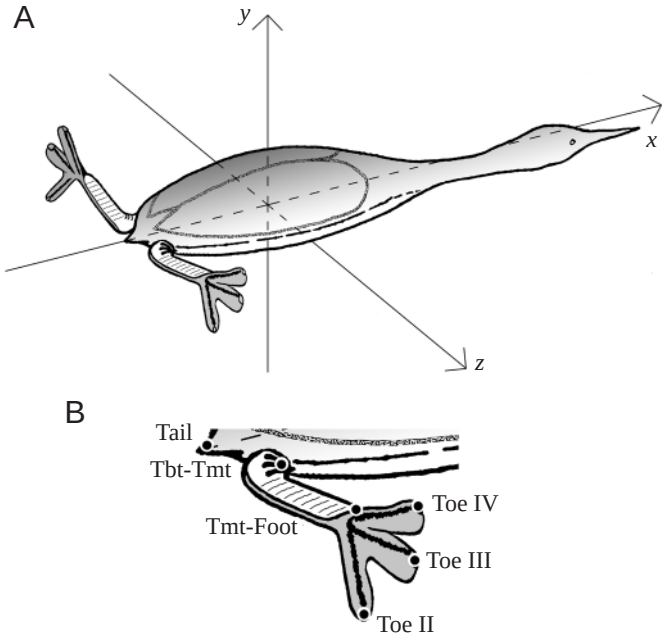

Fig. 1. (A) Schematic drawing of a great crested grebe (*Podiceps cristatus*) with the orientation of the reference grid (*x*, *y*, *z*) indicated. (B) Part of the body and leg to show the position of the measured points. Tail, tip of the tail; Tbt-Tmt, the joint between the tibiotarsus and tarsometatarsus; Tmt-Foot, the joint at the apical end of the tarsometatarsus; Toes II, III and IV, the tips of the three main toes. The lateral toe (toe IV) leads during the power stroke.

speed and ν is kinematic viscosity) based on the total body length of the bird (from the tip of the beak to the tail tip). A least-squares regression coefficient for the 13 sequences was calculated for mean stroke frequency *versus* mean swimming speed, and the slope was tested for significance using a Student's *t*-test.

Results

When submerged, the great crested grebe swam with synchronized foot strokes, keeping its wings closely folded against the body. Video images of the swimming grebe are shown in Fig. 2. The lateral (*x*, *y*) and dorsal (*x*, *z*) views of the movements of the six digitized points (Tail, Tbt-Tmt, Tmt-Foot and Toe II, III and IV), relative to the water, are plotted in Fig. 3. The movement paths of the measured points (for one of the analysed sequences), relative to that of the tail tip (fixed body point) in the three different planes, are plotted in Fig. 4. The movements of Tmt-Foot and the three toes, as between-frame displacements in the *x*, *y* and *z* directions, are shown in Fig. 5.

Power stroke

The power stroke, defined as the period during which the bird accelerates during a complete stroke, starts when the bird has its lowest speed in a stroke cycle (frame 5 in Figs 2–4) and ends when the bird reaches its highest speed (frames 10/11 in Figs 2–4). The power stroke represents 24±1.8 % (mean ± S.E.M., N=12) of the entire stroke duration irrespective of the swimming speed (P>0.69). During the power stroke, the feet moved from a cranial and ventrolateral position, with the outer toe (toe IV) leading, to a caudal and dorsomedial position relative to the body. The toes (of the right foot) move upwards (increasing *y*) and medially (decreasing *z*) relative to still water, but not backwards (constant *x*) (Figs 3, 5). The power stroke is initiated when the toes still have some forward movement relative to still water (Fig. 5). At the initiation of the power stroke, the toes start moving dorsally and then keep moving dorsally throughout most of the power stroke. The power stroke ends just before the toes reach their medialmost position, at which point the toes have already started to move ventrally (Fig. 4).

Recovery stroke

According to our definition of the power stroke, the recovery stroke is initiated just before the toes reach their medialmost position. As observed by Stolpe (Stolpe, 1935), at the beginning of the recovery stroke, the third and fourth toes rotate 90 ° around their own axis while folding. The second toe, which is almost perpendicular to the fourth toe during the power stroke, is folded to a position behind the tarsometatarsus in line with the other toes. The first part of the recovery stroke (frames 12–16) is characterized by a downward (decreasing *y*) and forward (increasing *x*) motion of the tarsus and foot, with a slow outward motion (increasing *z* for the right foot) relative to still water (Figs 3–5). The foot is then moved forwards along a ventrolateral path. During this part of the recovery stroke (frames 17–24 and frames 0–3), the toes move forward at an approximately constant velocity along the *x* axis and with slowly decreasing height (*y*). At the end of the recovery stroke (frames 3–5), the Tmt-Foot point slows its forward motion (relative to still water) and starts moving dorsally (increasing *y*). Just before the power stroke, the Tmt-Foot point also moves laterally as a result of dorsal extension of the tarsus. At the end of the recovery stroke, the toes extend laterally (increasing *z*), but they do not become fully extended until the power stroke is initiated (Figs 4A, 5).

Speed and amplitude

The mean swimming speed varied between 0.7 and 1.2 m s^{-1}, which gives a calculated Reynolds number *Re* for the bird's body of approximately 5×10^5. Stroke frequency

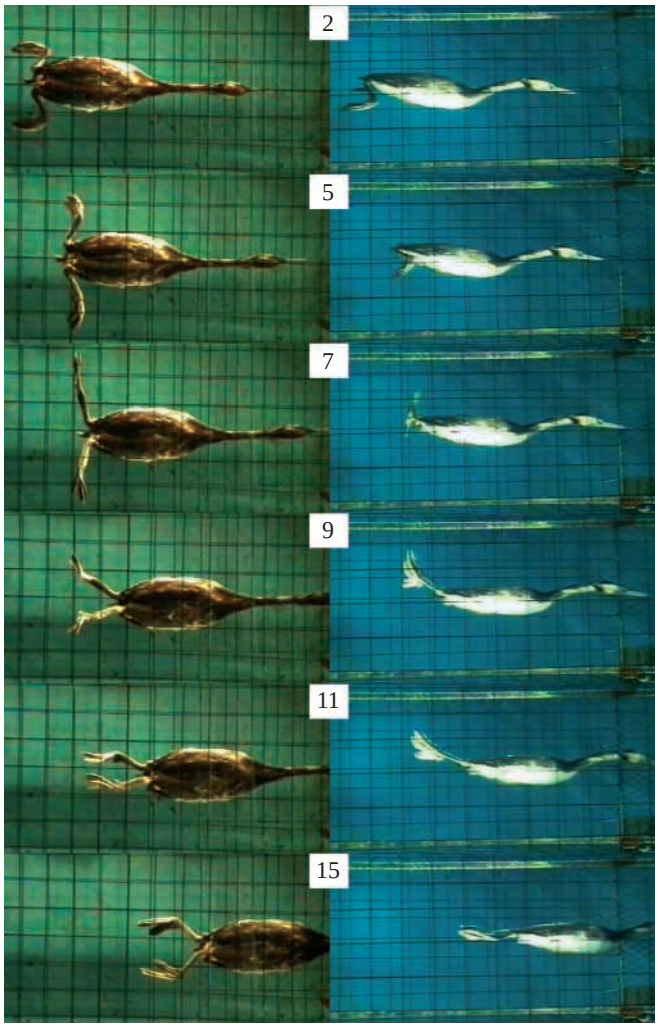

Fig. 2. Dorsal (left) and lateral (right) video frames of a diving grebe. The frame numbers correspond to the numbers in the graphs of Figs 3–5. Note that the tips of the toes do not move backwards during the power stroke (between frames 5 and 10/11), although the body of the bird is moving forwards. The dorsal view was recorded after reflection in a 45 ° mirror.

increased significantly with increasing swimming speed V (f=1.41V+0.90, P<0.05, r^2=0.57, N=13) (Fig. 6). However, there was no significant increase in stroke amplitude (of the Tmt-Foot point) with swimming speed [mean amplitude for the x axis 10.0±0.21 cm (P>0.51), for the z axis 4.43±0.14 cm (P>0.22) and for the y axis 8.45±0.22 cm (P>0.57); means ± S.E.M., N=13].

Lift-based propulsion

On the basis of the kinematics, it is possible to conduct a force/vector analysis to predict the direction of the lift and drag of the feet during the power stroke. Conventionally, drag is taken to be directed opposite to and lift perpendicular to the motion of the toes relative to still water (Vogel, 1994). The kinematics allows us to judge whether the angle of attack of the whole foot and at least toe IV is clearly positive or negative, and we can then determine the main direction of lift. The angles of attack of toes II and III are more strongly influenced by the flow around the other toes than is that of toe IV (see below), and it is therefore more difficult to estimate the angle of attack for these toes. Unfortunately, it is difficult to obtain a more precise estimate of the angle of attack for the toes during the power stroke from the video sequences and, therefore, a reliable estimate of the size of the forces could not be obtained. During the first part of the power stroke, the resultant force will be directed forwards and downwards, and during the last part it will be directed forwards and laterally and either downwards or upwards depending on the relationship between lift and drag. The feet are beaten synchronously, so all lateral forces will cancel, and the resultant force (over the entire power stroke) will be directed forwards and downwards/upwards (Fig. 7).

Our results indicate that the propulsive mechanism of the great crested grebe is based on hydrodynamic lift. The power stroke of the grebe, relative to still water, is in a plane more-or-less perpendicular to the direction of motion of the bird, indicating that the propulsive force is generated by hydrodynamic lift rather than drag.

Morphology

The tarsus has a width-to-depth ratio of 0.30 (Table 1), which is the same as a fineness ratio (length/maximum width of a body) of 3.3. For bodies of equal volume, the lowest resistance (at Re=10^7) is achieved by a streamlined body with a fineness ratio of 4.5, and for bodies of equal frontal area with a fineness ratio of 2 (Alexander, 1983). The asymmetry of the

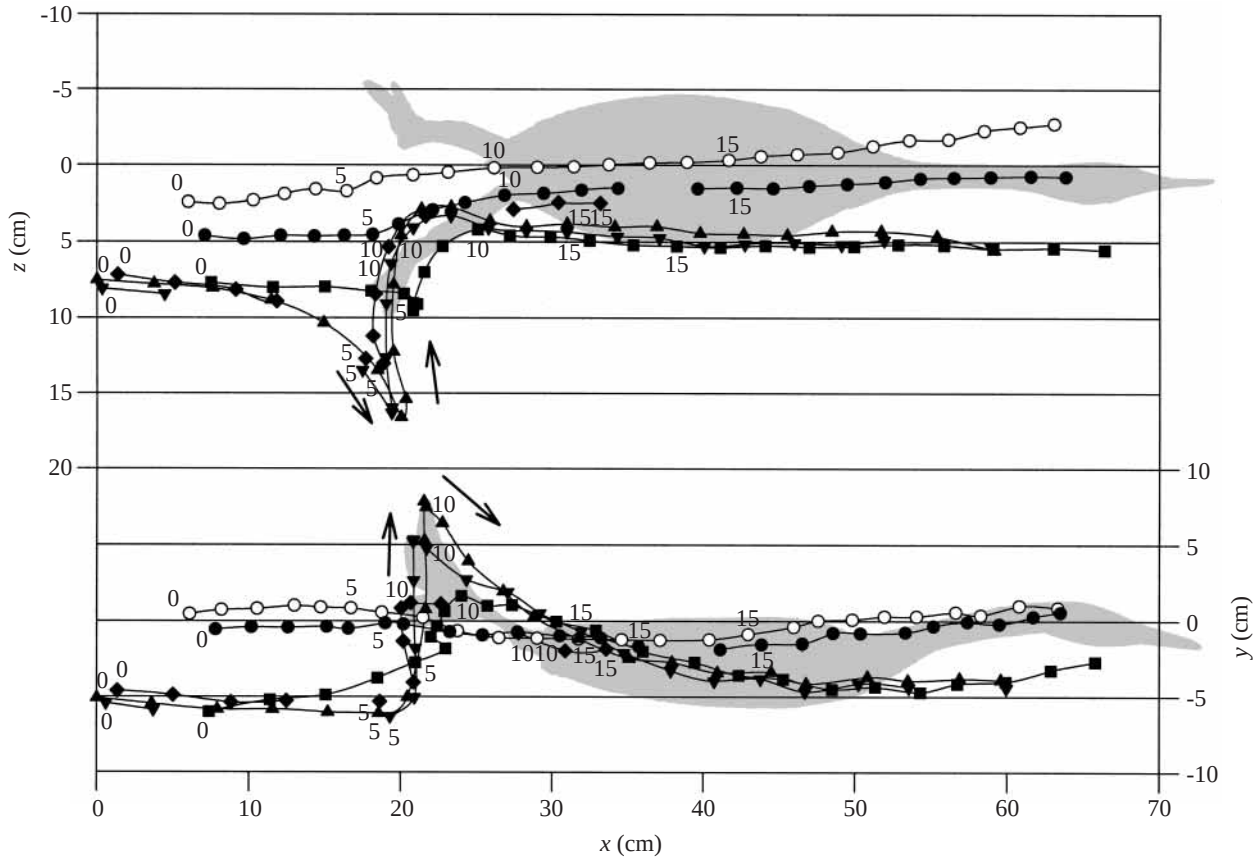

Fig. 3. Lateral (x, y plane) and dorsal (x, z plane) views of one sequence of a diving grebe relative to still water. The symbols mark the positions of digitized points: ○, Tail; ●, Tbt-Tmt; ■, Tmt-Foot; ◆, Toe II; ▼, Toe III; ▲, Toe IV (see Fig. 1B for definitions). Numbers in the graph correspond to frame numbers. During the power stroke (frames 5–10/11), the toes move through a large displacement in the z direction (towards the medial plane of the bird) and the y direction (upwards) but very little in the x direction (backwards or forwards).

grebe's toes at one-quarter of the toe length from the tips is close to that in the handwing feathers of flying birds; in both, the axis of rotation (where the toe phalanges and feather shaft are situated) lies approximately one-fifth to one-third of the chord length from the leading edge. Toe IV shows the greatest asymmetry and toe II the least. Toe IV is also the longest of the three largest toes and toe II the shortest (Table 1).

Discussion

It has been assumed that the power stroke of foot-propelled divers is drag-based rather than lift-based (Dabelow, 1925; Blake, 1981; Braun and Reif, 1985). The basis for drag-based propulsion is that the propulsive appendages move in a direction opposite to the swimming direction during the power stroke with a speed (relative to the body) greater than the swimming speed (Vogel, 1994). In the tufted duck (*Aythya fuligula*), a drag-based swimmer, the feet move caudally during the power stroke at an average speed of 1.56 times the speed of the bird while swimming at the surface (Woakes and Butler, 1983). The facts that the power stroke of the grebe is directed perpendicular to the swimming direction and that its toes do not move in a direction opposite to the swimming direction (relative to the water) during the power stroke strongly support the hypothesis of lift-based propulsion.

Speed limitations and energetics

In both drag-based and lift-based paddling, the maximum swimming speed depends on the maximum stroke frequency and the maximum stroke amplitude (the length of the traversed arc). The combination of these factors determines the velocity of the foot, which in turn determines the force produced. The angle of attack is an additional factor, together with stroke frequency and stroke amplitude, that limits lift-based paddling. The resultant velocity of the foot relative to still water is the vector sum of the velocity of the foot relative to the bird and the forward velocity of the body (Fig. 7). In spite of this similarity, the resulting maximum swimming speeds of the two systems differ because of the difference in stroke plane. In drag-based paddling, the feet are beaten parallel to, but in the opposite direction to, the swimming direction of the bird, which requires that the feet move backwards (relative to the bird) faster than the forward velocity of the bird to generate a propulsive force (Vogel, 1994, pp. 284–285) (see above). The

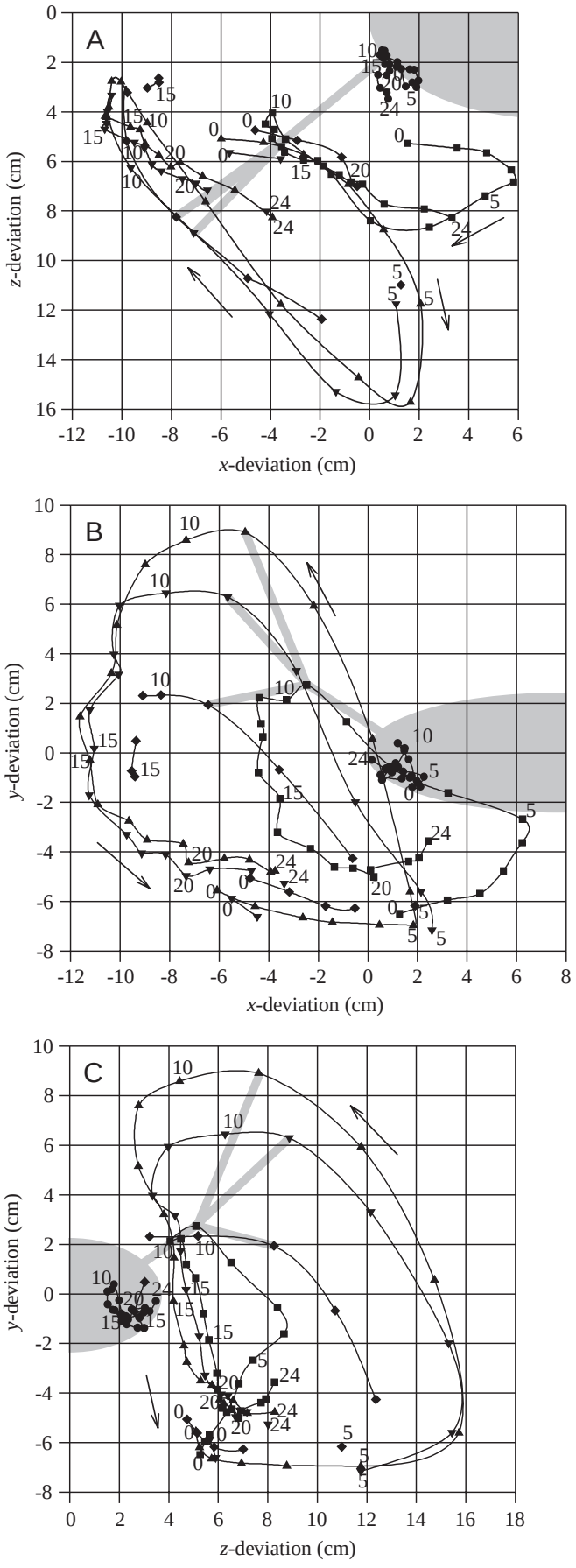

Fig. 4. (A) Dorsal view (*x*, *z* plane), (B) lateral view (*x*, *y* plane) and (C) caudal view (*z*, *y* plane) of foot movement relative to that of the tail tip. ●, Tbt-Tmt; ■, Tmt-Foot; ◆, Toe II; ▼, Toe III; ▲, Toe IV (see Fig. 1B for definitions). Numbers in the graph correspond to frame numbers. The power stroke extends from frame 5 to frames 10/11. In C, because of the use of separate cameras to capture the dorsal and lateral views, synchronization of the measurements of the two planes is not exact. Therefore, there is a small error in the relative timing of the *z* and *y* coordinates in this figure. This does not affect the interpretation of the results. The grey shaded region in each part represents the position of the leg and part of the grebe's body near the end of the power stroke (frame 9).

bird cannot swim faster than the speed of the foot stroke. In lift-based paddling, in contrast, the force produced is less tightly linked to the swimming speed of the bird. The stroke plane of the feet relative to still water is perpendicular to the swimming direction. This does not mean that the lift-based system is independent of swimming speed. Instead, the forward swimming velocity (**V** in Fig. 7) and the velocity of the foot ($\mathbf{V_b}$ in Fig. 7) do not cancel each other, as in drag-based propulsion, but change the direction of the flow across the foot (Fig. 7).

The direction from which the resultant velocity vector ($\mathbf{V_r}$ in Fig. 7) meets the foot (angle of attack, α) determines the direction of the resulting force by affecting the ratio of lift to drag (Norberg, 1990; Vogel, 1994). The maximum speed at which it is possible to produce a force in the swimming direction (thrust) depends strongly on the angle of attack at which the appendages can be held and on the direction and velocity of the flow across the foot relative to the swimming direction. In the grebe, the foot stroke itself produces most of the flow across the foot, but in forward flight, the forward motion of the bird generates a substantial amount of the flow across the wings (Dickinson, 1996). Therefore, it should be expected that the stroke frequency and/or the stroke amplitude of the swimming grebe should increase with increasing swimming speed. In fact, the stroke frequency of the grebe

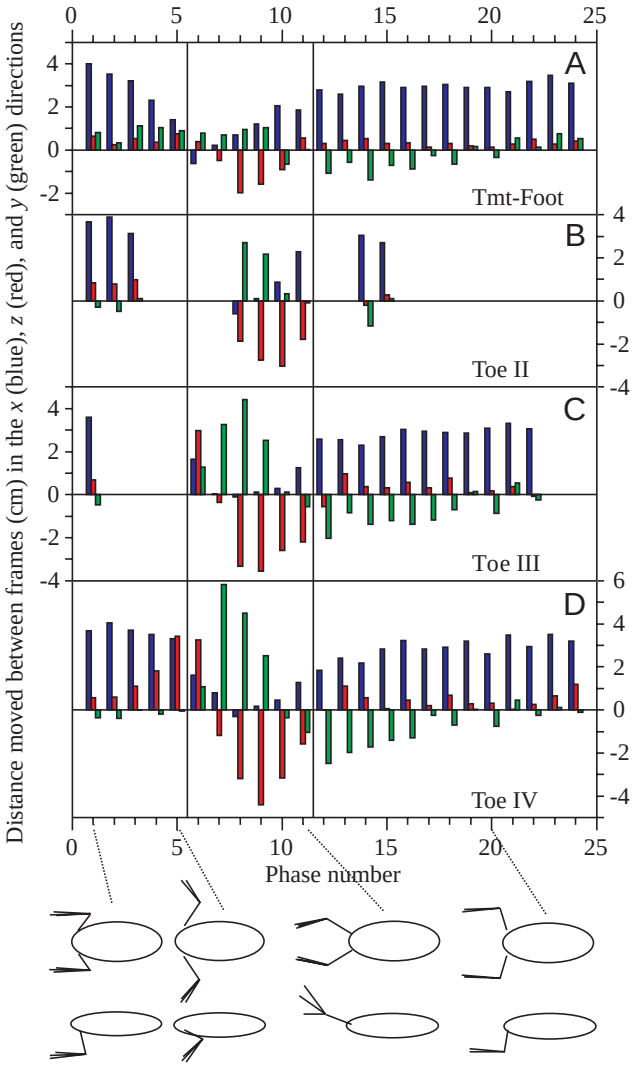

Fig. 5. Distance moved between frames in the *x* (blue), *z* (red) and *y* (green) directions relative to the still water and the bird's line of motion for the digitized points: Tmt-Foot (A), Toe II (B), Toe III (C) and Toe IV (D). The *x* axis shows the phase number (for example, 6 is the distance travelled between frame 5 and frame 6; as used in Figs 2–4). The vertical lines define the power stroke (phases 6–11). Line-drawings at the bottom of the figure show the position of the legs at the indicated phase (frame) for the dorsal (upper) and lateral (lower) views. The distance moved in the *x* direction is the average of the *x* distances measured in the dorsal and lateral planes. The time between each phase is 0.02 s.

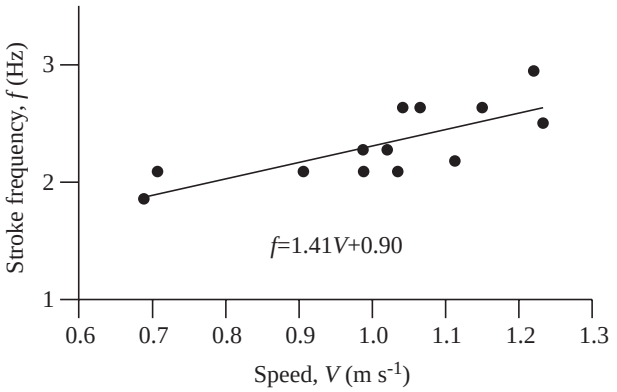

Fig. 6. Stroke frequency *f versus* mean horizontal swimming speed *V* of a great crested grebe. Frequency is positively correlated with speed ($P<0.05$, $r^2=0.57$, $N=13$).

Table 1. *Morphometric measurements of great crested grebes (*Podiceps cristatus*)*

Variable	Bird in our study	Other specimens
Body mass (kg)	0.8	0.57–1.49
Body length (cm)	46	
Tarsus length (cm)	6.6 (1)	5.7–7.1
Tarsus width/depth (%)	30±0.55 (2)	27±0.37 (8)
Foot area (cm^2)	25.7±0.78 (2)	29.4±1.4 (8)
Toe length (cm)		
Toe II	5.10±0.075 (2)	5.74±0.10 (8)
Toe III	7.30±0.085 (2)	7.05±0.18 (8)
Toe IV	7.54±0.025 (2)	7.18±0.15 (8)
Toe asymmetry lateral lobe/toe chord (%)		
Toe II	41±1.2 (2)	38±1.1 (8)
Toe III	23±1.3 (2)	25±0.7 (8)
Toe IV	16±0.8 (2)	17±1.5 (8)

Values are means ± S.E.M. (*N*), where *N* is the number of feet studied.

Body mass and tarsus length of the other specimens are from Cramp and Simmons (1977); all other data are our own measurements.

Body length was measured from video images.

increases with speed (Fig. 6), although we found no statistically significant increase in the amplitude of the *x*, *y* or *z* directions with increasing swimming speed for the joint between the tarsometatarsus and the foot.

Another aspect of drag-based *versus* lift-based paddling is the difference in energetic efficiency. The paddling motion of the grebe is very similar to the wing-paddle motion of racing kayaks. As in kayak paddling with a wing-blade, the grebe produces propulsion by fluid-dynamic lift and has a non-propulsive recovery stroke. A large proportion of the motion of the kayak paddle is normal to the track of the hull, and this results in a vortex larger than that produced by a normal 'drag' paddle (Jackson et al., 1992). A larger vortex has a lower core velocity, which is more efficient (Rayner, 1979). Lift-based paddling is more efficient than drag-based paddling (Jackson et al., 1992), suggesting that the lift-based paddling of the grebe is an energy-saving adaptation.

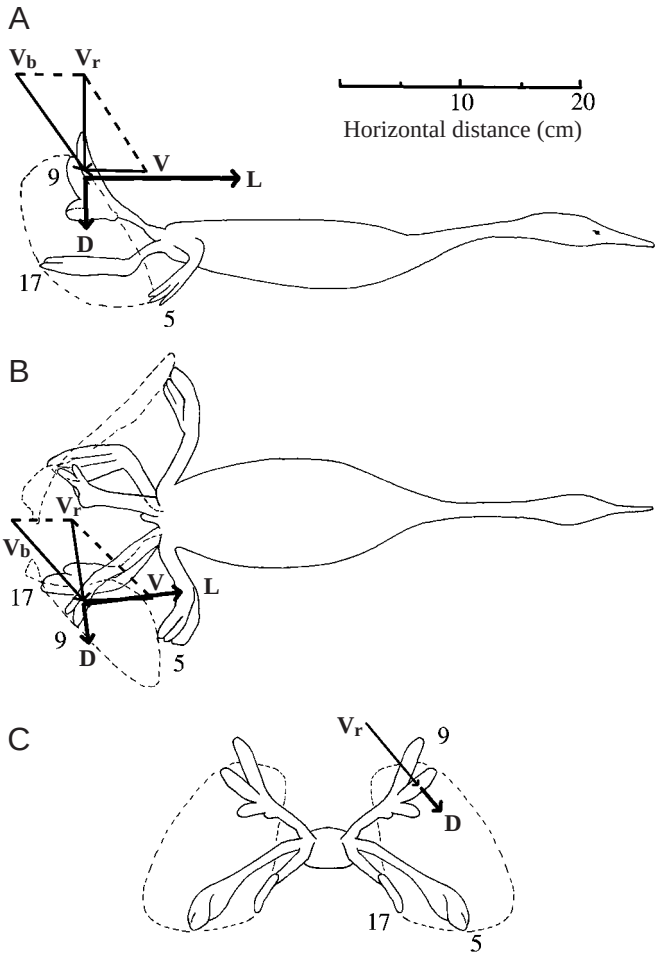

Fig. 7. Lift (**L**) and drag (**D**) forces and velocities acting on the foot of the grebe during different phases of the foot stroke when swimming at 1.15 m s^{-1}. The magnitudes of the lift and drag forces are arbitrary, and *L*/*D* is taken to be 5. The relative magnitudes of the velocities are measured as the distance travelled from two frames back to the present (i.e. over 0.04 s). **V** is the velocity of the forward motion of the bird, $\mathbf{V_b}$ is the velocity of the motion of the toes relative to the bird and $\mathbf{V_r}$ is the resultant velocity (the velocity of the water relative to the feet). Lateral (A), dorsal (B) and posterior (C) projections of the foot movements relative to the body. Three different positions of the legs are shown in each case (the numbers refer to the frame numbers in Figs 2–5). During the power stroke (here represented by frame 9), the toes are spread and the feet move upwards, backwards and inwards, resulting in a forward-directed lift force (**L**) and an outward and downward directed drag force (**D**). During the recovery stroke (represented by frame 17), the toes are folded and moved forwards. At the bottom of the turning phase (represented by frame 5), the toes begin to move laterally, with the edge of the fourth toe meeting the oncoming water.

Functional morphology

The lobed toes of the grebe may function as multiple slots (Johansson and Lindhe Norberg, 2000), increasing hydrodynamic/energetic efficiency, maximum lift and lift-to-drag ratio and decreasing drag production. To be able to function as a multiple-slotted hydrofoil, the toes must be separated perpendicular to the direction of the oncoming water (staggered), as in flying birds and aeroplanes (Hummel, 1980). In fact, this is the case in diving grebes (Fig. 3). The effects of staggered winglets at the wingtips have been tested in wind tunnels (for a review, see Hofton, 1978). The greatest reductions in induced drag (drag due to lift production) were achieved with three or four short winglets, with the anteriormost one pointing slightly upwards and the posteriormost one slightly downwards. Multiple slots in the wings of, for example, soaring birds could increase the lift-to-drag ratio of the wing by as much as 107 % by decreasing the induced drag (Tucker, 1993). In swimming grebe, an increase in the lift-to-drag ratio is of importance because it determines the direction of the resulting propulsive force (see above).

Asymmetrical lobing of the toes has also been assumed to be an adaptation to rotate the toes passively to minimize drag during the recovery stroke (Stolpe, 1935). We have suggested that it might be an adaptation to self-stabilize the toes during the power stroke (Johansson and Lindhe Norberg, 2000); experiments with single feet with cut-off tendons have shown that lateral separation and staggering of the toes can be achieved passively under hydrodynamic load. In multiple-slotted wings of aeroplanes, the centre of pressure of the anteriormost winglet is situated more anteriorly than that of the second and third winglets, with the third winglet having its centre farthest back of the three elements (Smith, 1975). If the axis of rotation of the wing of an aeroplane or feather is situated along the centre of pressure when the aerofoils operate at optimal angles of attack, then they are in equilibrium. Any deviation from this optimal angle of attack would result in a shift in the position of the centre of pressure, which in turn would result in a rotating moment working to bring the system back to equilibrium (described in rotating samaras by Norberg, 1973). The asymmetry occurring in the handwing feathers of flying birds is an adaptation for this self-stabilization during flight (Norberg, 1985). If the grebe's toes do act as multiple slots, then this would be greatly favoured by different degrees

of asymmetry of the toe lobings, with the greatest asymmetry on the toe leading the movement during the power stroke (toe IV). The toe leading the motion is indeed the most asymmetrical (Table 1), just as the primaries closest to the leading edge of the wing show the highest asymmetry in birds (Norberg, 1985; Norberg, 1990).

An important function of separated primary feathers is that the flight feathers act as separate aerofoils, each producing lift and each twistable individually in the nose-down direction under aerodynamic load. The separated feathers can be twisted more than the entire wingtip with unseparated feathers and, thereby, maintain similar local angles of attack along the entire length of the feathers and, hence, favourable lift coefficients. The toes of the great crested grebe function in a similar way. The rotating motion of the foot (Fig. 4C) results in a velocity gradient along the toes, with increasing velocity from the bases to the tips (Fig. 5). An aero/hydrofoil has different optimal angles of attack at different velocities but, more importantly, the velocity gradient changes the local direction of the oncoming water. Therefore, one would expect that the toes would be twisted to maintain optimal angles of attack along their entire length during the power stroke (like the blades of a propeller). If this twisting is to be achieved passively, the asymmetry should increase towards the tips of the toes, which is indeed the case, at least for toes II and III (Johansson and Lindhe Norberg, 2000).

Force production

Our definition of the power stroke depends on the problem of defining the turning points in the different directions, because it is a three-dimensional motion. At the end of the conventional power stroke (excursion in the *x* direction), the feet of this bird move little in the *x* direction and quite a lot in the *y* direction (Fig. 4B). The consequence of this would be a quite arbitrary calculation of the duration of the power stroke (analogous to finding a shallow maximum on a curve). Of course, it is possible that a forward force is produced after the power stroke (as defined by us), which is smaller than the drag of the bird. We think it unlikely that this force is based on drag, because, during this phase, the bird has its maximum forward velocity and it would be hard for the bird to move its feet faster than the swimming speed (i.e. move backwards relative to the water). In fact, it is clear from Fig. 5 that the feet have a considerable forward speed relative to still water during this part of the stroke.

The motion of the feet can be compared with that of asymmetrical hovering in birds (other than hummingbirds), in which the power stroke (or more precisely the period between the formation of the starting vortex and the stopping vortex) is represented by the downstroke and the recovery stroke by the upstroke. In both a hovering bird and a diving grebe, the motion of the propulsive appendage generates the fluid movement across the aero/hydrofoil, and very little or none of the flow is due to the motion of the body through the fluid (see above). Furthermore, the motion of the feet of the grebe and the wingstroke of a hovering bird are rotary, which means that

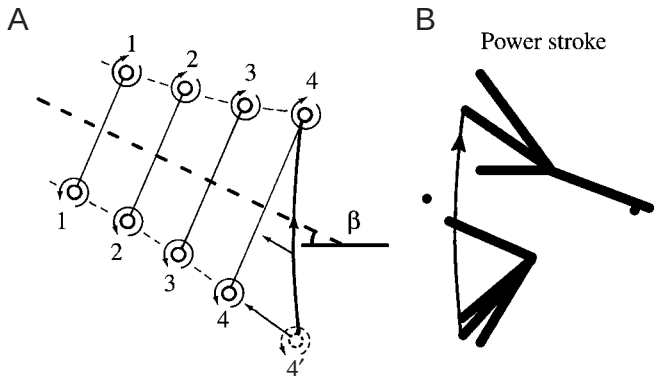

Fig. 8. (A) Lateral view of a schematic pattern of a vortex street for the diving bird, assuming that the flow pattern resembles that of asymmetrical hovering. The numbers represent successive power strokes, and β is the angle between the vortex street and the horizon. (B) The position of the legs at the start (bottom) and end (top) of the power stroke. The filled circles indicate the positions of the tail tip.

the feet sweep a sector-shaped area during the power stroke, making momentum jet theory applicable to the flow generated. It is likely that the grebe produces a vortex ring/street tilted slightly upwards (Fig. 8), resulting in a propulsive force directed forwards and slightly downwards. The resultant force would have to overcome the drag of the bird, the resistance due to the acceleration reaction and also the upward force of the bird's buoyancy to keep the bird on a level swimming path at a constant speed. If the hydrodynamics of diving grebes is similar to the aerodynamics of hovering flight, the separated toes make sense. The main contributor to the power requirements of hovering and slow flight is induced drag (Norberg, 1990), which can be reduced by multiple aero/hydrofoils (as discussed above).

Concluding remarks

Only one or two strokes could be observed every time the bird passed the measuring section of the tunnel, which made it somewhat difficult to determine whether the strokes observed were representative of the specific speeds recorded. In fact, in all our sequences, the bird followed the same kinematic pattern. The kinematics of the great crested grebe in this study resembles the motion described in the same species by Frank and Nue (Frank and Nue, 1929) and the motion both of captured wild birds filmed in our facility and of birds observed in water tanks in a zoological garden in Silkeborg, Denmark. The quality of our films of the wild birds was not sufficient for the detailed analysis required here.

The observed speed of our tame bird (approximately $1\,m\,s^{-1}$) was similar to speeds of great crested grebes observed in the wild (Bolam, 1921; Harrisson and Hollom, 1932). The Reynolds number (5×10^5) was close to those found for other diving birds and swimming animals, such as medium-sized fish (Webb, 1988; Lovvorn et al., 1991). In our study, the stroke frequency increased with increasing swimming speed, which agrees with results for other swimming birds (Woakes and Butler, 1983; Baudinette and Gill, 1985). An increase in stroke

amplitude instead of, or as well as, an increase in stroke frequency has been found in mallard ducklings (*Anas platyrhynchos*) and tufted ducks (*Aythya fuligula*) (Woakes and Butler, 1983; Aigeldinger and Fish, 1995). A few of these studies concern surface swimming, which may be very different because the feet are mostly beaten alternately.

Grebes spend most of their time in or on the water and have almost lost their ability to walk on land (Harrisson and Hollom, 1932). The consequence should be that conflicting selection pressures for both walking and swimming/diving would be reduced in favour of selection for purely swimming and diving. The Podicipediformes is an old group of birds with no close living relatives (Sibley and Ahlquist, 1990), and yet their morphological features have remained more or less unchanged since at least the Oligocene (Storer, 1960) and maybe even since the end of the Cretaceous (Cooper and Penny, 1997), suggesting that the grebes have been under stabilizing selection. Stolpe (Stolpe, 1935) has suggested that at least the fourth toe of *Hesperornis* functioned mechanically in the same manner as the toes of the grebes. This makes sense only if the toe was asymmetrically lobed. If it was, this suggests that *Hesperornis* might have used the same locomotor mechanism as the grebes. Lift-based paddling might therefore represent a local evolutionary maximum in foot-propelled swimming.

It would be of interest to assess the efficiency of lift-based paddling compared with wing-propelled diving, although we expect underwater flight to be more efficient because of the unproductive recovery stroke of lift-based paddling.

We are indebted to Richard Brown for giving support and inspiration, to Anna Zeffer for taking care of the bird and to three anonymous referees for valuable comments on the manuscript. We also thank Pernilla Jonsson and Mikael Thollesson for comments on an early version of the manuscript. This study was funded by The Swedish Natural Science Research Council (to U.M.L.N.), the H. Ax:son Johnson foundation, the E. Colliander foundation, the Royal and Hvitfeldska foundation, the Royal Swedish Academy of Science (Regnell and Hierta-Retzius) and the W. and M. Lundgren foundation (all to L.C.J.).

References

Aigeldinger, T. L. and Fish, F. E. (1995). Hydroplaning by ducklings: overcoming limitations to swimming at the water surface. *J. Exp. Biol.* **198**, 1567–1574.

Alexander, R. McN. (1983). *Animal Mechanics.* Funtington: Packard Publishing Limited. 301pp.

Baudinette, R. V. and Gill, P. (1985). The energetics of ‘flying’ and ‘paddling’ in water: locomotion in penguins and ducks. *J. Comp. Physiol.* B **155**, 373–380.

Blake, R. W. (1981). Mechanics of drag-based mechanisms of propulsion in aquatic vertebrates. *Symp. Zool. Soc. Lond.* **48**, 29–52.

Bolam, G. (1921). Rate of progress of great crested grebe under water. *Brit. Birds* **14**, 189.

Braun, J. and Reif, W.-E. (1985). A survey of aquatic locomotion in fishes and tetrapods. *N. Jahrb. Geol. Paläont. Abh.* **169**, 307–332.

Brooks, A. (1945). The under-water actions of diving ducks. *Auk* **62**, 517–523.

Carbone, C., De Leeuw, J. J. and Houston, A. I. (1996). Adjustments in the diving time budgets of tufted duck and pochard: is there evidence for a mix of metabolic pathways? *Anim. Behav.* **51**, 1257–1268.

Cooper, A. and Penny, D. (1997). Mass survival of birds across the Cretaceous–Tertiary boundary: Molecular evidence. *Science* **275**, 1109–1113.

Cracraft, J. (1982). Phylogenetic relationships and monophyly of loons, grebes and Hesperornithiform birds, with comments on the early history of birds. *Syst. Zool.* **31**, 35–56.

Cramp, S. and Simmons, K. E. L. (1977). *Handbook of the Birds of Europe, the Middle East and North Africa: the Birds of the Western Palearctic*, vol. 1, *Ostrich to Ducks.* Oxford: Oxford University Press. 722pp.

Cramp, S. and Simmons, K. E. L. (1983). *Handbook of the Birds of Europe, the Middle East and North Africa: the Birds of the Western Palearctic*, vol. 3, *Waders to Gulls.* New York: Oxford University Press. 913pp.

Dabelow, A. (1925). Die Schwimmanpassnung der Vögel. Ein Beitrag zur biologischen Anatomie der Fortbewegung. *Jb. Morph. Mikroskop. Anat.* **54**, 288–321.

Dickinson, M. H. (1996). Unsteady mechanics of force generation in aquatic and aerial locomotion. *Am. Zool.* **36**, 537–554.

Fish, F. E. (1996). Transitions from drag-based to lift-based propulsion in mammalian swimming. *Am. Zool.* **36**, 628–641.

Frank, H. R. and Nue, W. (1929). Die Schwimmbewegnungen der Tauchvögel (Podiceps). *Z. Vergl. Physiol.* **10**, 410–418.

Harper, P. C., Croxall, J. P. and Cooper, J. (1985). A guide to foraging methods used by marine birds in Antarctic and Subantarctic seas. *Biomass Handbook* **24**, 1–22.

Harrisson, T. H. and Hollom, P. A. D. (1932). The great crested grebe enquiry. *Brit. Birds* **26**, 142–155.

Hofton, A. (1978). How sails can save fuel in the air. *New Scient.* 20 April, 146–147.

Högman, S. (1873). *Jemförande Framställning af Skelettbyggnaden hos Colymbus och Podiceps*. Upsala: Akademiska Boktryckeriet. 40pp.

Hummel, D. (1980). The aerodynamic characteristics of slotted wing-tips in soaring birds. In *Proceedings of the 17th Ornithological Congress*, vol. 1 (ed. R. Nöhring), pp. 391–396. Berlin: Verlag der Deutchen Ornithologen-Gesellschaft.

Jackson, P. S., Locke, N. and Brown, P. (1992). The hydrodynamics of paddle propulsion. In *11th Australasian Fluid Mechanics Conference* (ed. M. R. Davis and G. J. Walker), pp. 1197–1200. Hobart: University of Tasmania.

Johansson, L. C. and Lindhe Norberg, U. M. (2000). Asymmetric toes aid underwater swimming. *Nature* **407**, 582–583.

Lovvorn, J. R. (1994). Biomechanics and foraging profitability: an approach to assessing trophic needs and impacts of diving ducks. *Hydrobiologia* **279/280**, 223–233.

Lovvorn, J. R. and Jones, D. R. (1991). Effects of body size, body fat and change in pressure with depth on buoyancy and costs of diving in ducks (*Aythya* spp.). *Can. J. Zool.* **69**, 2879–2887.

Lovvorn, J. R., Jones, D. R. and Blake, R. W. (1991). Mechanics of underwater locomotion in diving ducks: drag, buoyancy and acceleration in a size gradient of species. *J. Exp. Biol.* **159**, 89–108.

Norberg, R. Å. (1973). Autorotation, self-stability and structure of single-winged fruits and seeds (samaras) with comparative remarks on animal flight. *Biol. Rev.* **48**, 561–596.

Norberg, R. Å. (1985). Function of vane asymmetry and shaft curvature in bird flight feathers; inferences on flight ability of *Archaeopteryx*. In *The Beginnings of Birds, Proceedings of the International* Archaeopteryx *Conference Eichstätt 1984* (ed. M. K. Hecht, J. H. Ostrom, G. Viohl and P. Wellnhofer), pp. 303–318. Eichstätt: Freunde des Jura-Museums Eichstätt.

Norberg, U. M. (1990). *Vertebrate Flight: Mechanics, Physiology, Morphology, Ecology and Evolution.* Berlin, Heidelberg, New York: Springer Verlag. 291pp.

Nue, W. (1931). Die Schwimmbewegungen der Tauchvögel (Blässhuhn und Pinguine). *Z. Vergl. Physiol.* **14**, 682–708.

Owre, O. T. (1967). Adaptations for locomotion and feeding in the Anhinga and the Double-crested cormorant. *Orn. Monogr.* **6**, 1–138.

Raikow, R. J. (1970). Evolution of diving adaptations in the stifftail ducks. *Univ. Calif. Publ. Zool.* **94**, 1–52.

Rayner, J. M. V. (1979). A vortex theory of animal flight. Part 2. The forward flight of birds. *J. Fluid Mech.* **91**, 731–763.

Rosser, B. W. C., Secoy, D. M. and Riegert, P. W. (1982). The leg muscles of the American coot (*Fulica americana* Gmelin). *Can. J. Zool.* **60**, 1236–1256.

Sibley, C. G. and Ahlquist, J. E. (1990). *Phylogeny and Classification of Birds: A Study in Molecular Evolution.* New Haven: Yale University Press. 976pp.

Smith, A. M. O. (1975). High lift aerodynamics. *J. Aircraft* **12**, 501–530.

Stephenson, R. (1994). Diving energetics in lesser scaup (*Aythya affinis*, Eyton). *J. Exp. Biol.* **190**, 155–178.

Stephenson, R., Lovvorn, J. R., Heieis, M. R. A., Jones, D. R. and Blake, R. W. (1989). A hydromechanical estimate of the power requirements of diving and surface swimming in lesser scaup (*Aythya affinis*). *J. Exp. Biol.* **147**, 507–519.

Stolpe, M. (1935). Colymbus, Hesperornis, Podiceps: ein Vergleich ihrer hinteren Extremität. *J. Orn.* **83**, 115–128.

Storer, R. W. (1960). Adaptive radiation in birds. In *Biology and Comparative Physiology of Birds*, vol. 1 (ed. A. J. Marshall), pp. 15–55. New York: Academic Press.

Tome, M. W. and Wrubleski, D. A. (1988). Underwater foraging behavior of Canvasbacks, Lesser scaups and Ruddy ducks. *Condor* **90**, 168–172.

Townsend, C. W. (1909). The use of wings and feet by diving birds. *Auk* **26**, 234–248.

Tucker, V. A. (1993). Gliding birds: reduction of induced drag by wing tip slots between the primary feathers. *J. Exp. Biol.* **180**, 285–310.

Vogel, S. (1994). *Life in Moving Fluids.* Princeton, NJ: Princeton University Press. 467pp.

Webb, P. W. (1988). Simple physical principles and vertebrate aquatic locomotion. *Am. Zool.* **28**, 709–725.

Wilcox, H. H. (1952). The pelvic musculature of the loon, *Gavia immer*. *Am. Midl. Nat.* **48**, 513–573.

Woakes, A. J. and Butler, P. J. (1983). Swimming and diving in tufted ducks, *Aythya fuligula*, with particular reference to heart rate and gas exchange. *J. Exp. Biol.* **107**, 311–329.